



## Removal of copper through adsorption by magnesium hydroxide nanorod

Jianwen Hao<sup>a,\*</sup>, Chenwei Dai<sup>a</sup>, Yongchun Liu<sup>a,b</sup>, Qing Yang<sup>a,b</sup>

<sup>a</sup>Department of Chemical Engineering, Anhui Vocational and Technical College, Hefei 230011, China, Tel. +86-551-64689841; Fax: +86-551-64689999; emails: haojw@mail.ustc.edu.cn (J. Hao), dddcccwww@163.com (C. Dai), 2875346727@qq.com (Y. Liu), 1021565210@qq.com (Q. Yang)

<sup>b</sup>Department of Chemical and Materials Engineering, Hefei University, Hefei 230022, China

Received 28 February 2017; Accepted 7 September 2017

### ABSTRACT

In this study, the magnesium hydroxide nanorod (MHN) was successfully prepared by precipitation–recrystallization method, which was chartered with X-ray diffraction, transmission electron microscope and scanning electron microscope. In view of superiority, MHN was used as adsorbent to adsorb copper ions from wastewater. A range of tests in regard to the effect of initial  $\text{Cu}^{2+}$  ion concentration, initial solution pH value, contact time and MHN dosage on adsorption of  $\text{Cu}^{2+}$  ion from wastewater were investigated. The results revealed the investigated factors which can have a profound effect on adsorption of  $\text{Cu}^{2+}$  ion. The adsorption capacity reached about 250 mg/g within 50 min, showing that MHN had rapid adsorption effect to  $\text{Cu}^{2+}$  ion. By fitting three kinetic equations, the pseudo-second-order kinetic equation was found to fit the best adsorption behavior. The analysis of equilibrium isotherm proved that the adsorption behavior was in accordance with the Langmuir equation, and MHN had favorable adsorption capacity to copper ion (324 mg/g and 318 K). The obtained thermodynamic data exhibited that the adsorption behavior was viable, initiative and endothermic, and the degree of disorder was increasing. The testing on MHN regeneration was evaluated by desorbing the MHN copper-adsorbed in 0.1 M NaCl solution or 0.1 M sodium ethylenediaminetetraacetic acid (EDTA) solution. The removal efficiency after eight cycles still reached to 75% for regeneration with EDTA treatment. In conclusion, the presented results demonstrated the potential use of MHN in adsorbing copper ion from wastewater because of its speediness, high adsorption capacity and recyclability.

*Keywords:* Copper; Magnesium hydroxide; Nanorod; Adsorption; Kinetics; Thermodynamics

### 1. Introduction

Due to the rapid development of society, a large amount of industry, such as coating, metallurgy, chemical engineering, dyes and electronics, extensively take copper-based compound as raw materials, and a large number of wastewater containing copper ion is directly discharged [1]. Nevertheless, copper is acutely toxic, and non-biodegradable to aquatic ecosystems and living organisms [2]. Also, copper is able to accumulate in sediments and tissues of living organisms. Hence, to avoid polluting environment, the separation of copper ions is essential to before discharging wastewater into environment.

There are many treatment methods to be utilized in copper removal, such as coagulation [3], flocculation [4], bioremediation [5], advance oxidation processes [6], membrane separation [7] and adsorption [8]. Compared with other methods, adsorption is effective technology for treating low-concentration wastewater containing heavy metals and favorable to use as advanced treatment for emission up to standard. On the other hand, adsorption technology has low operation and maintenance costs in removing heavy metals in dilute solutions. Thus, various adsorbents have been utilized for adsorbing metal ions, for instance, active carbon [9], clay [10], ash [11], chitosan [12], silica [13], zeolite [14], hydroxyapatite [15] and biosorbent [16]. Magnesium hydroxide, as an adsorbent, has the characters of great buffer ability, better activity, high adsorption performance, safety,

\* Corresponding author.

non-toxic, harmless and high activity [17,18]. Magnesium hydroxide can be also widely prepared by many methods and is a relatively cheap adsorbent. Hence, it is regarded as a green adsorbent and has been employed to treat wastewater in the past few years [17–20]. Nevertheless, the researches on magnesium hydroxide nanomaterials as adsorbent for adsorbing copper ion are less reported.

Here, we report a strategy to fabricate magnesium hydroxide nanorod (MHN) for adsorbing copper ion in wastewater. Subsequently, adsorption properties were also investigated in detail. The effects of initial  $\text{Cu}^{2+}$  ion concentrations, initial solution pH value, contact time and adsorbent dosage on adsorption performance were investigated. Three models, namely, the pseudo-first-order equation, the pseudo-second-order equation and the intra-particle diffusion equation, were discussed for adsorption kinetics. For adsorption equilibrium research, Langmuir and Freundlich isotherms model were utilized. The parameters on adsorption thermodynamic were also computed and discussed. Regeneration of MHN was also evaluated by soaking the MHN copper-adsorbed in 0.1 M NaCl solution or 0.1 M sodium ethylenediaminetetraacetic acid (EDTA) solution.

## 2. Materials and methods

### 2.1. Materials

$\text{MgSO}_4 \cdot 7\text{H}_2\text{O}$  and NaOH was used for preparing MHN and  $\text{CuSO}_4 \cdot 5\text{H}_2\text{O}$  was used for preparing copper-containing simulation wastewater in the paper. Sodium EDTA was used as complexing agent, acetic acid and sodium acetate was used for making up buffer solution in spectrophotometric technology based on the complex reaction. All used chemicals were obtained from Shanghai Chemical Reagent Co. Ltd., China, and of analytical pure. The corresponding solutions were prepared by dissolving the chemicals in deionized water or absolute ethyl alcohol. Deionized waters were used throughout.

### 2.2. Preparation of magnesium hydroxide nanorod

MHN was synthesized by precipitation method [20]. In the course of preparation, 31.25 g of  $\text{MgSO}_4 \cdot 7\text{H}_2\text{O}$  was dissolved in 260 mL water, and 1.4 g of NaOH was dissolved in 80 mL ethanol. Under magnetic stirring,  $\text{MgSO}_4$  solution was dropwise added into NaOH solution at 85°C, and kept on stirring for 24 h. Then, the precipitate was obtained by vacuum filtration, and purified with deionized water and ethanol for removing additional impurities. The precursors were prepared after dried at 60°C for 24 h. The obtained precursors were added in 160 mL 1.25 mol/L NaOH solutions and stirred at 80°C for 2 h. The samples were filtered, and purified by deionized water and ethanol. In the end, after dried at 60°C for 24 h, the MHN samples were obtained.

### 2.3. Characterization of MHN

The crystal formation of obtained MHN was characterized by X-ray diffraction (XRD). The XRD peaks were tested on an X-ray diffractometer by utilizing CuK radiation (40 kV, 2,500 v/pc, 200 mA; D/max rA model, Hitachi, Japan) in the range of 5°–70° at the speed of 2°/min.

The microstructural characterization of MHN samples was tested with transmission electron microscope (TEM) with an electron acceleration voltage of 200 kV (200CX model, JEOL, Japan) and scanning electron microscope (SEM) with an electron acceleration voltage of 5 kV (Sirion 200, FEI, Holland).

The specific surface area and porosity were measured by  $\text{N}_2$  adsorption–desorption isotherms at 77 K using a surface area and porosity analyzer (TriStar II 3020, Micromeritics, USA).

The  $\text{pH}_{\text{zpc}}$  value of MHN samples was tested by a micro-electrophoretic mobility detector (DXD-II model, Jiangsu Optical Industrial Co., China).

### 2.4. Adsorption experiments

The simulation wastewaters were obtained by dissolving quantitative copper sulfate pentahydrate ( $\text{CuSO}_4 \cdot 5\text{H}_2\text{O}$ ) into deionized water. After diluting synthetic wastewaters, a series of solution for adsorption testing were obtained. Through small batch experiments, the adsorption studies of  $\text{Cu}^{2+}$  ion onto MHN were investigated. The quantitative MHN was added to 100 mL solution containing  $\text{Cu}^{2+}$  ion of desired concentrations. The processes were performed in 250 mL Erlenmeyer flasks by mixing  $\text{Cu}^{2+}$  ion solution and MHN. The analyses of  $\text{Cu}^{2+}$  ion were performed with spectrophotometric technology based on the complex reaction between  $\text{Cu}^{2+}$  ion and EDTA. The spectrophotometric technology was achieved in pH 5.5 of buffer solution. The concentration of used EDTA was 8%. The absorption wavelength was 735 nm, and the time of complex reaction was set 5 min. The tests were conducted in triplicate for obtaining reproductive results with deviation error smaller than 5%. If the deviation error is higher than 5%, more experiments were performed. Hence, the experimental data can be repeated with accuracy larger than 95%. The data listed in this work are the average values of three tests.

For investigating the effects of experimental conditions onto the adsorption of  $\text{Cu}^{2+}$  ion, the variation of MHN dosage (0.2–1.4 g/L), contact time (5–50 min), pH (1–8) and initial  $\text{Cu}^{2+}$  ion concentration (5–85 mg/L) were conducted. The other fixed conditions were listed in the related figure captions.

The effects of initial  $\text{Cu}^{2+}$  ion concentration (5–85 mg/L) and varying temperature (298, 308 and 318 K) onto the  $\text{Cu}^{2+}$  ion adsorption were tested for studying adsorption isotherm, while MHN dosage, contact time and pH is fixed at 1.0 g/L, 50 min and 6, respectively.

The effects of contact time (5–50 min) and varying initial  $\text{Cu}^{2+}$  ion concentration (25, 50 and 55 mg/L) onto the  $\text{Cu}^{2+}$  ion adsorption were used for the kinetic experiments, while initial  $\text{Cu}^{2+}$  ion concentration, MHN dosage and pH is fixed at 60 mg/L, 1.0 g/L and 6, respectively.

### 2.5. Regeneration of MHN

The regeneration performance of MHN was investigated with desorption in 0.1 M NaCl or 0.1 M sodium EDTA solutions, respectively. First, the copper-loaded MHN was desorbed in 0.1 M sodium EDTA or 0.1 M NaCl solution along with oscillation in room temperature for 1 h, purified with distilled water and dried in vacuum condition in room temperature for 2 h. Subsequently, the adsorption efficiency of

MHN was tested again for copper ions. As above adsorption and desorption treatment, eight consecutive cyclic operations were tested for evaluating the regeneration performance of MHN.

### 2.6. Calculations

The  $\text{Cu}^{2+}$  ion removal efficiency (%) was computed according to the following formula:

$$\text{Removal efficiency (\%)} = \frac{(C_i - C_e)}{C_i} \times 100\% \quad (1)$$

The quantity of  $\text{Cu}^{2+}$  ion adsorbed at equilibrium was computed according to the following formula:

$$q_e = \frac{(C_i - C_e)V}{m} \quad (2)$$

where  $q_e$  (mg/g) is the quantity of  $\text{Cu}^{2+}$  ion adsorbed at equilibrium,  $V$  (L) is the wastewater bulk,  $m$  (g) is the mass of MHN.  $C_i$  (mg/L) and  $C_e$  (mg/L) are the initial and equilibrium  $\text{Cu}^{2+}$  ion concentrations, separately.

## 3. Results and discussion

### 3.1. Characterization of materials

The XRD pattern of obtained MHN is revealed in Fig. 1. Compared with the standard peaks (JCPDS 07-0239), all diffraction peaks are sharp and consistent well with standard peaks of magnesium hydroxide hexagonal system. In addition, the peaks belonged to other impurities are not discovered in Fig. 1. It reveals that the MHN are well crystallized and highly purified.

The morphology and structure of the MHN is investigated by TEM and SEM, as shown in Figs. 2 and 3, respectively. As seen from TEM image and SEM, MHN has a rod shape with particle diameters of between 50 and 100 nm and lengths of about 1  $\mu\text{m}$ . While the crystallite diameter calculated with Scherrer formula based peak width from XRD is about 20 nm [20]. Also, the particle diameter is wider than

crystallite diameter. It can be explained that the MHN particle is composed of little crystallites agglomeration. Beyond that, it is also seen that some pores with a pore size of about 50 nm are exposed in MHN. SEM of MHN after desorption

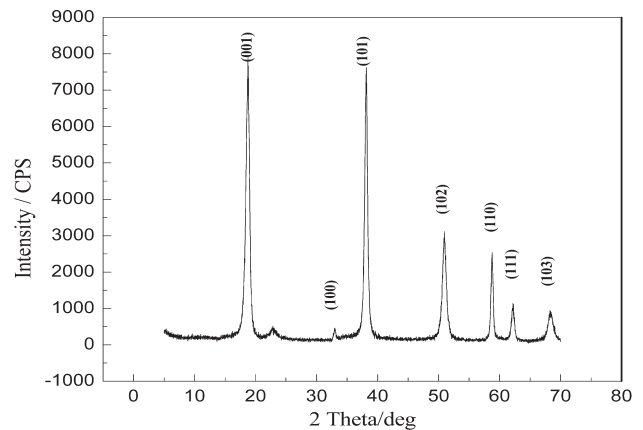


Fig. 1. XRD pattern of MHN.

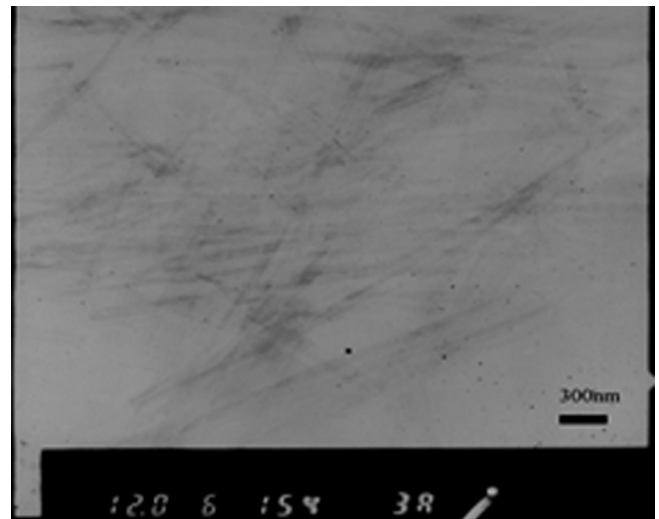


Fig. 2. TEM image of MHN.

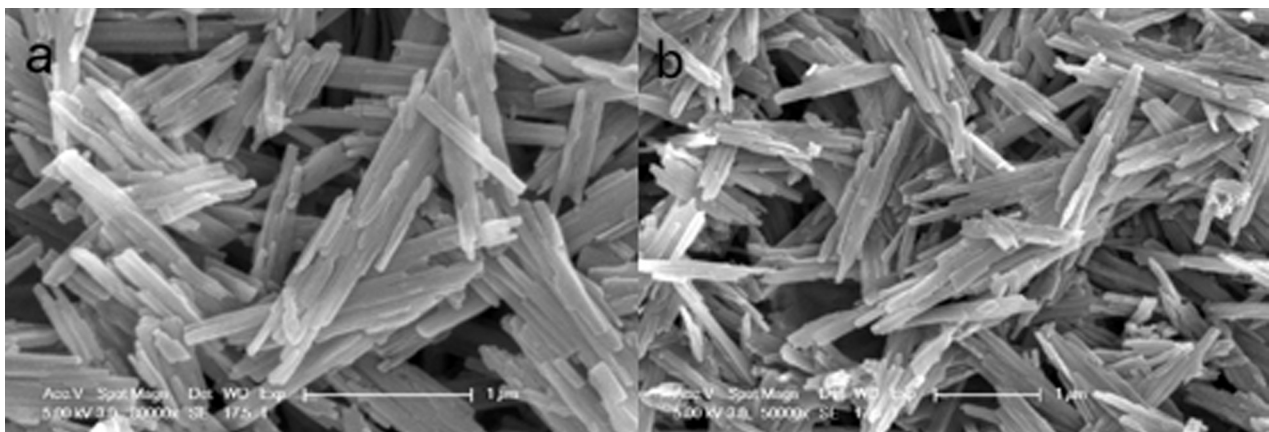


Fig. 3. SEM image of MHN (a) before adsorption and (b) after desorption.

also can be obtained in Fig. 3(b). As shown in Fig. 3(b), the morphology of MHN after desorption has a little change but still maintains rod-like. This shows that the structure of MHN can remain stable throughout adsorption.

The tested specific surface area value of MHN is 100.6 m<sup>2</sup>/g, and the tested porosity value of MHN is 0.34. They are close to those of other reported study [17,20].

### 3.2. Effect of adsorption factors

#### 3.2.1. Effect of MHN dosage

The influence of MHN dosage on Cu<sup>2+</sup> ion removal efficiency is displayed in Fig. 4. As shown in Fig. 4, the removal efficiency first keeps constantly increasing with the added MHN dosage. The reason is that the raise of adsorbent particles number apparently matches the growth of available adsorption sites [21]. As a result, more Cu<sup>2+</sup> ions are attached to the surfaces of MHN particles. Subsequently, the removal percentage increases slowly and reaches gradually 100% until the MHN dosage beyond 1.0 g/L, in which the equilibrium is arrived. Therefore, 1.0 g/L is chose as adsorbent dose for further tests.

#### 3.2.2. Effect of contact time

Contact time can affect largely the rate of adsorption of Cu<sup>2+</sup> ion on the surface of MHN in adsorption process and is regarded as a vital factor to be investigated. The influence of contact time was shown in Fig. 5. As shown in the figure, the removal percentage of Cu<sup>2+</sup> ion is rapid initially with 30 min and then gradually become constant until the balance. During the rapid adsorption step, the Cu<sup>2+</sup> ions diffuse from the solution to the external surface of MHN, while in the slow adsorption step, the Cu<sup>2+</sup> ions diffuse from the external surface of MHN to the pores in MHN. In general, it is virtually impossible that the entire adsorption process is controlled by the external diffusion step under conditions of oscillation. Hence, it is deduced that the inner diffusion step controls entire adsorption process. While in the reported

works on adsorption of Cu<sup>2+</sup> ion with other bioadsorbents [22,23], the equilibrium time exceeds 500 min. Compared with other adsorbents, it shows that the adsorption of Cu<sup>2+</sup> ion with MHN rapidly arrives to equilibrium. The adsorption speed is rapid on account of the surface with massive active sites and high surface energy [24]. The speedy equilibrium time is a favorable advantage for adsorbing Cu<sup>2+</sup> ion. Hence, in order to ensure complete adsorption equilibrium, 50 min is selected as contact time in the subsequent testing.

#### 3.2.3. Effect of initial pH value

Obviously, the outside charge character of MHN and ionization degree of Cu<sup>2+</sup> ion can be impacted by the pH of solution [25–27]. Hence, it is evident that the adsorption characteristics are largely influenced by the pH value of solution [25–27]. As seen in Fig. 6, the adsorption quantity of Cu<sup>2+</sup>

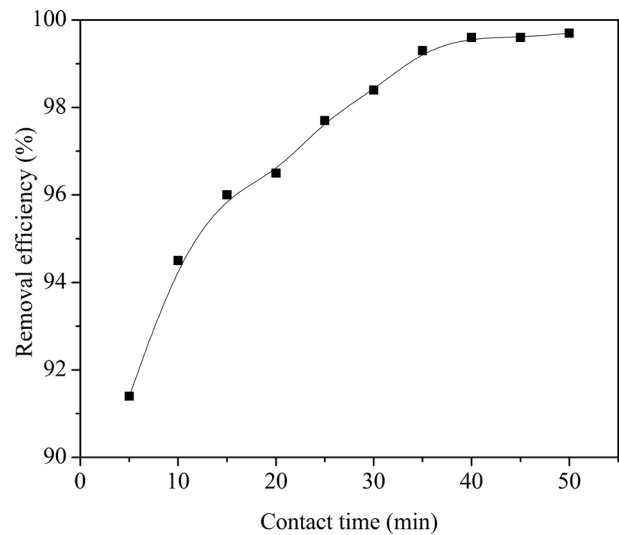


Fig. 5. Effect of contact time on removal efficiency (initial Cu<sup>2+</sup> ion concentration 60 mg/L, MHN dosage 1.0 g/L, T = 298 K and pH = 6).

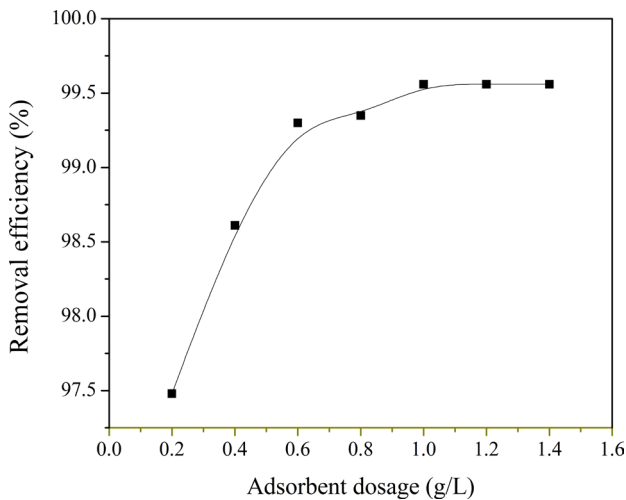


Fig. 4. Effect of MHN dosage on copper ion removal efficiency (initial Cu<sup>2+</sup> ion concentration 60 mg/L, contact time 50 min, T = 298 K and pH = 6).

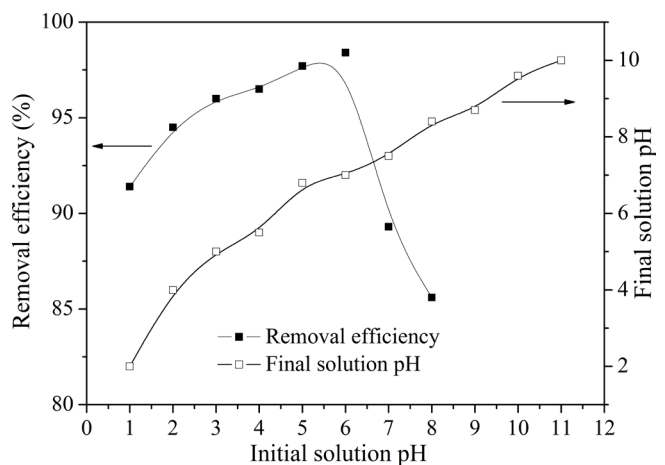


Fig. 6. Effect of initial pH value on removal efficiency and final solution pH (initial Cu<sup>2+</sup> ion concentration 60 mg/L, contact time 50 min, T = 298 K and MHN dosage 1.0 g/L).

ions adds fast along with the increased pH value from 1 to 6 and decreases along with the increased pH value from 6 to 8. When the solution pH is selected to 6.0, the maximum removal efficiency of copper ion is obtained. During lower pH value condition, the free  $\text{Cu}^{2+}$  ion is predominant form in adsorption experiments [28]. Meanwhile, because there are a lot of  $\text{H}^+$  ions existing in the solution, the surface of MHN readily adsorbs  $\text{H}^+$  ions and is protonated. This leads to positive charge in the surface of MHN [23]. Consequently, the concentration of  $\text{H}^+$  ions increases with decreasing initial pH value from 6.0 to 1, it can be deduced that the electrostatic repulsive force between positive charge on MHN surface and  $\text{Cu}^{2+}$  ion is enhanced with decreasing pH value from 6.0 to 1, and hence lesser  $\text{Cu}^{2+}$  ions are adsorbed by MHN. Nevertheless, when the pH value becomes higher, the concentration of  $\text{H}^+$  ions is reduced. It is accompanied by the increasing of  $\text{OH}^-$  ions in the adsorption solution, which is favored to form precipitate from copper hydroxide [20]. As a result, the removal efficiency decreases with increasing pH value from 6.0 to 8.0.

The point of zero charge, called  $\text{pH}_{\text{zpc}}$ , is the pH at which the zeta potential of adsorbent surface equals zero. It is generally adopted to qualitatively characterize the adsorbent surface charge. The charge on surface is a key role involved with adsorption chemistry. The pH is a crucial factor, which controls the surface charge of MHN. Hence, for confirming above assumption, the measured  $\text{pH}_{\text{zpc}}$  value of MHN is 10.1. In the above discussion on effect of initial pH value, the pH value ranges from 1 to 6, and is less than  $\text{pH}_{\text{zpc}}$ . Evidently, the surface of MHN is positively charged during the solution with pH 1–6, which may be expressed as  $\text{MHN}-\text{H}_3\text{O}^+$ . The positive charge increases with the pH decreases from 6 to 1. While the enhanced positively charge in  $\text{MHN}-\text{H}_3\text{O}^+$  is unfavorable for adsorption of the  $\text{Cu}^{2+}$  ion due to the intensive electrostatic repulsive-force between  $\text{MHN}-\text{H}_3\text{O}^+$  and  $\text{Cu}^{2+}$  ion. As a result, the  $\text{Cu}^{2+}$  ion removal efficiency gradually increases with the solution pH increases from 1 to 6, which verifies the above conjecture on adsorption mechanism in acidic condition.

The comparison between the initial and final pH value of  $\text{Cu}^{2+}$  ion adsorption experiments is also shown in Fig. 6. As seen in Fig. 6, MHN has a good pH buffering capacity. When the initial pH value is low, the final pH value is higher than initial pH value, which is ascribed to the dissolution of MHN. Also, at strongly acidic conditions,  $\text{H}^+$  ions are buffered by  $\text{OH}^-$  ions from dissolution of MHN. While the initial pH value is higher than 10, compared with the initial pH value, the final pH value decreases due to the adsorption of  $\text{OH}^-$  ions from the solution by MHN. Therefore, whatever the initial pH value,  $\text{H}^+$  ions or  $\text{OH}^-$  ions in solution can be buffered by MHN.

### 3.2.4. Influence of initial $\text{Cu}^{2+}$ ion concentration

The influence of  $\text{Cu}^{2+}$  ion concentration on the amount of  $\text{Cu}^{2+}$  ion adsorbed has been demonstrated in Fig. 7. It is visible that the quantity of  $\text{Cu}^{2+}$  ion adsorbed at equilibrium rises with the increasing initial concentration of  $\text{Cu}^{2+}$  ion from 5 to 60 mg/L, which can be ascribed to the quick augment of  $\text{Cu}^{2+}$  ion that occupying adsorption sites of MHN. While the initial concentration exceeds 60 mg/L, the quantity of  $\text{Cu}^{2+}$  ion

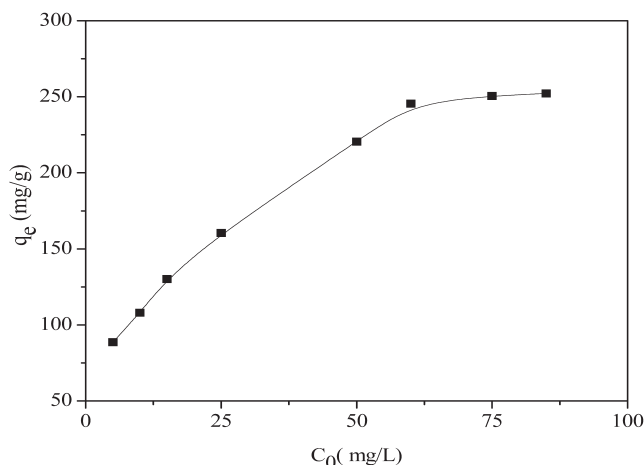


Fig. 7. Effect of initial  $\text{Cu}^{2+}$  ion concentration on the amount of  $\text{Cu}^{2+}$  ion adsorbed (MHN dosage 1.0 g/L, contact time 50 min,  $T = 298$  K and  $\text{pH} = 6$ ).

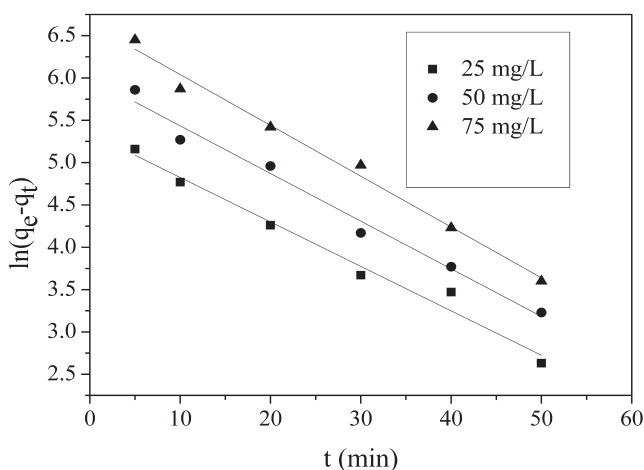


Fig. 8. Pseudo-first-order lines for adsorption of  $\text{Cu}^{2+}$  ion onto MHN (MHN dosage 1.0 g/L,  $T = 298$  K and  $\text{pH} = 6$ ).

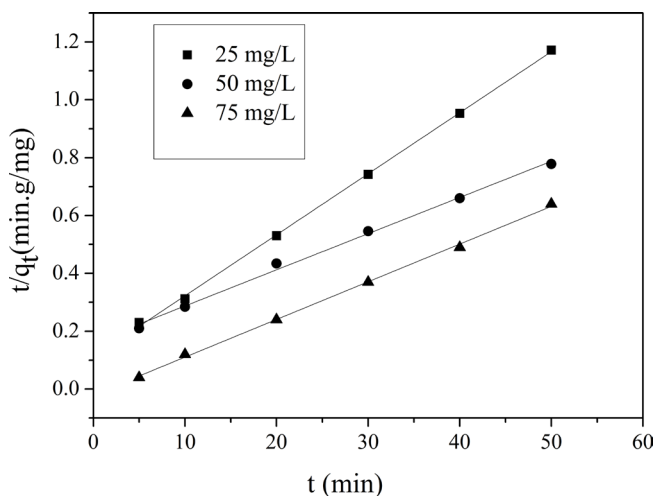


Fig. 9. Pseudo-second-order lines for adsorption of  $\text{Cu}^{2+}$  ion onto MHN (MHN dosage 1.0 g/L,  $T = 298$  K and  $\text{pH} = 6$ ).

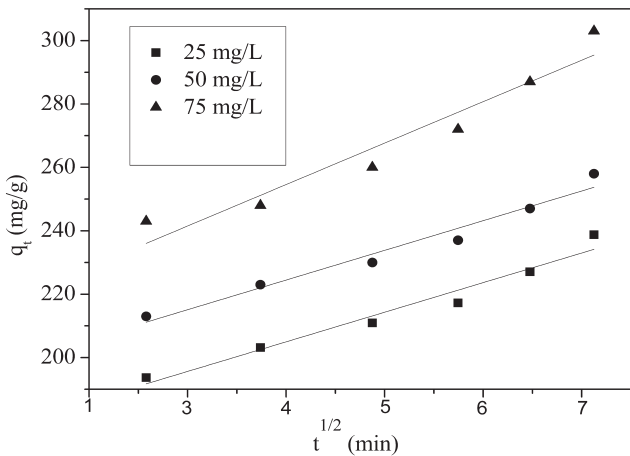


Fig. 10. Intra-particles diffusion lines for adsorption of Cu<sup>2+</sup> ion onto MHN (MHN dosage 1.0 g/L, T = 298 K and pH = 6).

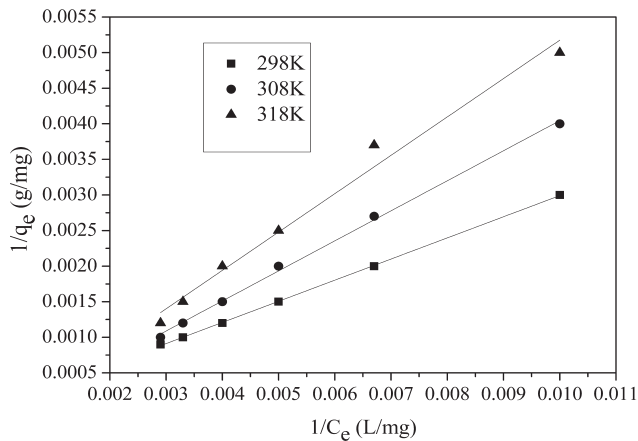


Fig. 11. Langmuir isotherm equation lines for adsorption of Cu<sup>2+</sup> ion on MHN (MHN dosage 1.0 g/L, contact time 50 min and pH = 6).

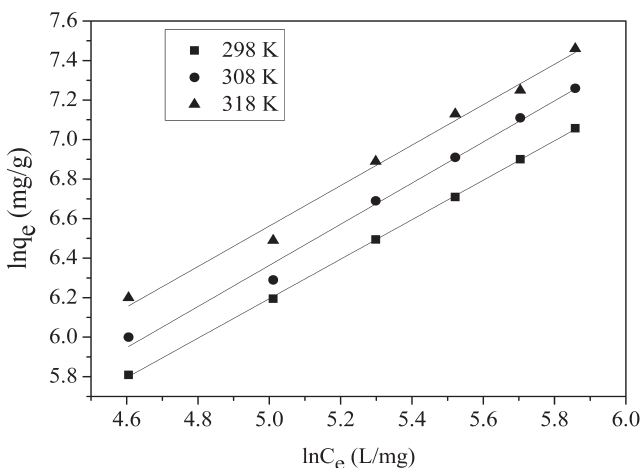


Fig. 12. Freundlich isotherm equation lines for adsorption of Cu<sup>2+</sup> ion on MHN (MHN dosage 1.0 g/L, contact time 50 min and pH = 6).

adsorbed at equilibrium keeps essentially constant. It can be due to the causes that excess Cu<sup>2+</sup> ion may lead to rapid equilibrium of MHN surface at higher concentration [29].

### 3.3. Adsorption kinetics

For estimating the adsorption rate and investigating the controlling mechanism of adsorption processes, kinetics is regarded as a considerable characteristic, which need be discussed in detail. Hence, several kinetic equations including the pseudo-first-order equation, pseudo-second-order equation and intra-particles diffusion equation are adopted to describe the adsorption process. The linear expression of three models is obtained as follows:

$$\ln (q_e - q_t) = \ln q_e - k_1 t \tag{3}$$

$$\frac{t}{q_t} = \frac{1}{q_e^2 k_2} + \frac{t}{q_e} \tag{4}$$

$$q_t = A + kt^{1/2} \tag{5}$$

where  $q_e$  (mg/g) and  $q_t$  (mg/g) are the adsorption quantities at equilibrium and at time  $t$  (min), respectively,  $k_1$  (min<sup>-1</sup>) and  $k_2$  (mg·g/min) are the rate constants of the pseudo-first-order equation and pseudo-second-order equation, respectively,  $k$  (mg·g·min<sup>-0.5</sup>) is the intra-particle diffusion rate constant and  $A$  is the intercept.

The related arguments of three kinetic models are fitted in Figs. 8–10 and shown in Table 1. The correlation coefficient ( $R^2$ ) and residual sum of square (RSS) can be employed as criterion for evaluating the fitting quality. According to Table 1, by comparing the correlation coefficient ( $R^2$ ) and RSS of three kinetic equations, the pseudo-second-order equation with higher  $R^2$  and lower RSS, is regarded to be extremely befitting model in matching the adsorption kinetics of Cu<sup>2+</sup> ion adsorption onto MHN. It proves that chemical interaction between MHN and Cu<sup>2+</sup> ion might take place in the adsorption process and is rate-limiting step. It is assumed that the adsorption probably occurs with surface reactions related with the number of active surface sites. In addition, it can also be discovered in Table 1 that the pseudo-second-order rate constant  $k_2$  lessens as the increased initial Cu<sup>2+</sup> ion concentration. These results are similar to the previous research involving Cu<sup>2+</sup> ion adsorbed onto other adsorbents [30,31].

### 3.4. Adsorption isotherms

Adsorption isotherms can be employed in explaining the equilibrium relationship between copper ion and MHN. The linear expression of two equations related to adsorption isotherms is obtained as follows:

$$\frac{1}{q_e} = \frac{1}{q_m k_L} \cdot \frac{1}{C_e} + \frac{1}{q_m} \tag{6}$$

$$\ln q_e = \frac{1}{n} \ln C_e + \ln k_f \tag{7}$$

where  $q_e$  (mg/g) is the amount of  $\text{Cu}^{2+}$  ion adsorbed by MHN;  $q_m$  (mg/g) is the maximum adsorption quantity of  $\text{Cu}^{2+}$  ion adsorbed by MHN.  $k_L$  (L/mg) is constant of the Langmuir isotherm equation,  $C_e$  (mg/L) is the concentration of the  $\text{Cu}^{2+}$  ion in solution.  $k_f$  and  $n$  are parameters of the Freundlich isotherm equation. The parameters of the Langmuir and Freundlich isotherm equations are fitted in Figs. 11 and 12 and shown in Table 2. By means of comparing the correlation coefficients ( $R^2$ ) and RSS, it is observed that the Langmuir isotherm equation with higher  $R^2$  and lower RSS is most fitted to illustrate the adsorption process. These results suggest that  $\text{Cu}^{2+}$  ion were adsorbed onto the MHN in a monolayer, which are in accordance with those previous researches about adsorption with magnesium hydroxide [21,32]. Although the correlation coefficients ( $R^2$ ) based Freundlich model are smaller than those of Langmuir model, it is also seen from Table 2 that the correlation coefficients ( $R^2$ ) of Freundlich model in all cases exceed 0.95. The Freundlich parameters  $n$  at 298, 308 and 318 K are 2.08, 2.24 and 2.31, respectively. The  $n$  value is in the range of 2–10, which forecasts adsorption course is favorable [33]. The saturated amount of the  $\text{Cu}^{2+}$  ion adsorbed by MHN at 298–318 K is 207–324 mg/g. As seen in Table 3,  $q_m$  values of MHN are higher than the previous adsorbents reported on  $\text{Cu}^{2+}$  ion removal, which show that MHN has higher adsorption capacity for  $\text{Cu}^{2+}$  ion removal. On the other hand, compared with other adsorbents, magnesium hydroxide possesses the characters of great buffer ability, better activity, high adsorption performance, safety, non-toxic, harmless [17–20], and is a relatively cheap and can be widely prepared by many ingredients [17–20]. Therefore, it is feasible that  $\text{Cu}^{2+}$  ion is removed from wastewater by MHN.

Moreover, based on Langmuir isotherm, the favorability of adsorption process is also judged with the constant called

separation factor ( $R_L$ ). It is calculated with the following equation:

$$R_L = \frac{1}{1 + k_L C_e} \quad (8)$$

where  $k_L$  (L/mg) is constant of the Langmuir isotherm equation. The parameter  $R_L$  is related to the shape of Langmuir isotherm:  $R_L > 1$  signifies that adsorption process is unfavorable,  $R_L = 1$  signifies that adsorption process is linear,  $0 < R_L < 1$  signifies that adsorption process is favorable,  $R_L = 0$  signifies that adsorption process is irreversible. The  $R_L$  values are obtained and listed in Table 2. As seen from Table 2,  $R_L$  values are 0.019–0.213, 0.021–0.270 and 0.024–0.295, when the temperature is 298, 308 and 318 K, respectively. It presents that the adsorption of  $\text{Cu}^{2+}$  ion onto MHN is favorable [20].

### 3.5. Adsorption thermodynamics

For purpose of investigating the thermodynamic possibility and identifying the characteristic of the adsorption

Table 3  
Comparison on adsorption capacity of different adsorbents

Adsorbent	Adsorption capacity (mg/g)	Reference
<i>S. platensis</i>	67.9	[34]
Activated carbon	30.8	[35]
Chitosan beads	52.6	[36]
Activated charcoal	21.2	[37]
Fish bones	150.7	[38]
Garden grass	58.34	[16]

Table 1  
A comparison of fitting results based three kinetic models at different initial copper ion concentration

Concentration (mg/L)	$q_{e,exp}$ (mg/g)	Pseudo-first-order equation				Pseudo-second-order equation			
		$k_1$ (min <sup>-1</sup> )	$q_{e,cal}$ (mg/g)	$R^2$	RSS	$k_2$ (mg·g/min)	$q_{e,cal}$ (mg/g)	$R^2$	RSS
25	145.6	0.02037	220.3	0.972	0.157	0.02363	145.6	0.991	0.105
50	245.1	0.01854	364.4	0.971	0.056	0.01678	245.1	0.994	0.046
75	250.6	0.01654	724.1	0.980	0.036	0.01364	250.6	0.990	0.022
Concentration (mg/L)	$q_{e,exp}$ (mg/g)	Intra-particles diffusion equation							
		$A$	$k$ (mg·g·min <sup>-0.5</sup> )	$R^2$	RSS				
25	145.6	176.9	4.67	0.955	0.857				
50	245.1	196.4	4.68	0.958	0.455				
75	250.6	215.4	6.53	0.956	0.854				

Table 2  
A comparison of parameters based Langmuir and Freundlich equation at different temperatures

Temperature (K)	Langmuir					Freundlich			
	$k_L$ (L/mg)	$q_m$ (mg/g)	$R_L$	$R^2$	RSS	$k_f$	$n$	$R^2$	RSS
298	0.614	207	0.019–0.213	0.989	0.108	15.8	2.08	0.964	0.135
308	0.542	237	0.021–0.270	0.988	0.036	13.5	2.24	0.956	0.146
318	0.478	324	0.024–0.295	0.982	0.020	10.9	2.31	0.962	0.065

process, the thermodynamic data involving change in standard free energy ( $\Delta G$ ), change in enthalpy ( $\Delta H$ ) and change in entropy ( $\Delta S$ ), are computed from the following formulas:

$$\Delta G = -RT \ln K_D \quad (9)$$

$$\ln K_D = \frac{\Delta S}{R} - \frac{\Delta H}{RT} \quad (10)$$

where  $K_D$  is distribution coefficient of  $\text{Cu}^{2+}$  ion between the MHN and solution at equilibrium (L/mol),  $R$  is the ideal gas constant (8.31 J/mol K) and  $T$  is the Kelvin temperature (K).  $\Delta H$  and  $\Delta S$  are obtained from the slope and intercept of van't Hoff plots of  $\ln K_D$  vs.  $1/T$ , respectively. The  $\Delta G$ ,  $\Delta H$  and  $\Delta S$  values are shown in Table 4.

In general, when the value of standard free energy is from  $-20$  to  $0$  kJ/mol, the adsorption process is judged to be physical adsorption. While its value changes from  $80$  to  $400$  kJ/mol, and it display that the adsorption process is chemical adsorption [39]. As shown in Table 4, the total  $\Delta G$  values are negative values from  $-6.78$  to  $-12.7$  kJ/mol and the overall  $\Delta H$  values are positive values. It reveals that the adsorption process is an autonomous physical adsorption and more beneficial in higher temperatures [39]. In addition, energy is adsorbed during adsorption process, which is also revealed in Table 4. It is seen that the change value of entropy is non-negative, showing that the randomness of adsorption process is increasing. The raising randomness may be explained by the releasing of  $\text{H}_2\text{O}$  molecules and  $\text{SO}_4^{2-}$  ions existed on the MHN surface in adsorption process.

### 3.6. Regeneration of the adsorbent

In consideration of economic efficiency, the reusability of adsorbent is a very important property and should be evaluated in industrial wastewater treatment process. Hence, it is necessary to detect the reusability of MHN. The procedures are conducted to regenerate the MHN adsorbed  $\text{Cu}^{2+}$  ion by soaking in the  $0.1$  M NaCl or  $0.1$  M EDTA solutions. Fig. 13 shows the MHN reusability by treating with above two solutions, respectively. For the MHN by EDTA treatment, it is observed that  $\text{Cu}^{2+}$  ion removal efficiency still arrives to  $75\%$  after eight cycles. While for the MHN by NaCl treatment, the  $\text{Cu}^{2+}$  ion removal efficiency is only  $70\%$  after one cycle. Hence, it is indicated that EDTA solution is more effective than NaCl solution for MHN regeneration. In the case of EDTA regeneration,  $\text{Cu}^{2+}$  ion can be effectively desorbed due to the strong complexation between  $\text{Cu}^{2+}$  ion and EDTA. While in the case of NaCl regeneration, the  $\text{Cu}^{2+}$  ion desorption is mainly achieved by exchanging  $\text{Cu}^{2+}$  ion with  $\text{Na}^+$  ion. In addition, when NaCl concentration is  $0.1$  M, the reduction of  $\text{Cu}^{2+}$  ion adsorption efficiency also may be ascribed to that salt effect is insufficiently strong to screen the electrostatic attraction between the positive  $\text{Cu}^{2+}$  ion and negative active adsorption site [25–27]. It results in relatively less  $\text{Cu}^{2+}$  ions desorption from MHN in NaCl solution. Therefore, desorption in  $0.1$  M EDTA is more effective than desorption in  $0.1$  M NaCl.

Table 4  
Thermodynamics parameters of  $\text{Cu}^{2+}$  ion adsorption process at different temperatures

Temperature (K)	$\Delta G$ (kJ/mol)	$\Delta H$ (kJ/mol)	$\Delta S$ (kJ/mol/K)
298	-6.78	54.5	208.6
308	-9.54		
318	-12.7		

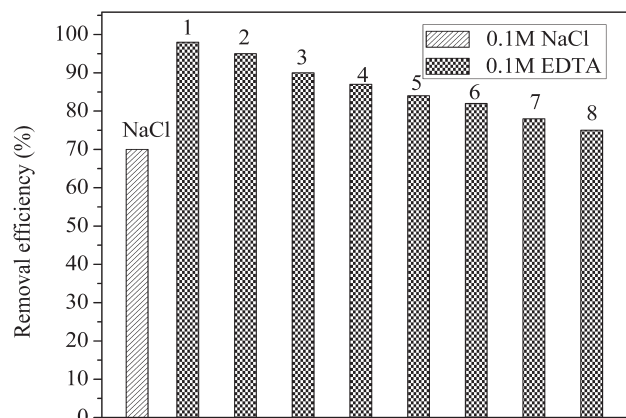


Fig. 13. Regeneration of MHN using  $0.1$  M NaCl and  $0.1$  M EDTA solutions.

## 4. Conclusion

In this study, MHN is successfully synthesized and characterized by XRD, SEM and TEM. For evaluating the adsorptive property, the MHN then is used for adsorbing  $\text{Cu}^{2+}$  ion in wastewater. The single-factor experiment results show that the adsorption of copper onto the MHN is considered to be profoundly depended on the initial  $\text{Cu}^{2+}$  ion concentration, pH value, contact time and adsorbent dosage. The removal rate reaches  $100\%$  within  $50$  min, and the highest adsorption quantity of MHN comes to  $324$  mg/g at  $318$  K, clearly revealing that MHN is effective and fast to adsorb copper ions from wastewater. Adsorption kinetics and isotherms are analyzed for further study. By comparing with three kinetic equations, these results demonstrate that adsorption kinetics is in accordance with the pseudo-second-order equation. On the other hand, it is shown that the Langmuir model is fit to express adsorption isotherms during the changed temperature. The thermodynamics data demonstrate that the adsorption process is viable, initiative and endothermic in essence. The augment of temperature favors adsorption process, which is also proved by thermodynamics data. Based on the circulatory test of desorption by  $0.1$  M EDTA and readsorption for  $\text{Cu}^{2+}$  ion, it suggests that MHN is promising and renewable adsorbent due to that  $\text{Cu}^{2+}$  ion removal efficiency still arrives to  $75\%$  after eight cycles.

## Acknowledgments

The work was funded by Key Project of Natural Science Foundation of Anhui Provincial Education Department (No. KJ2014A130) and Key Program for Excellent Young Talents in University of Anhui Provincial Education Department.



## Symbols

$C_e$	— Equilibrium $\text{Cu}^{2+}$ ion concentration, mg/L
$C_i$	— Initial $\text{Cu}^{2+}$ ion concentration, mg/L
$k$	— Rate constant of intra-particle diffusion equation, $\text{mg}\cdot\text{g}\cdot\text{min}^{-0.5}$
$k_1$	— Rate constant of the pseudo-first-order equation, $\text{min}^{-1}$
$k_2$	— Rate constant of the pseudo-second-order equation, $\text{mg}\cdot\text{g}/\text{min}$
$K_D$	— Distribution coefficient of $\text{Cu}^{2+}$ ion between the MHN and solution at equilibrium, L/mol
$k_F$	— Constant of Freundlich isotherm equation
$k_L$	— Constant of Langmuir isotherm equation, L/mg
$m$	— Mass of MHN, g
$q_e$	— Quantity of $\text{Cu}^{2+}$ ion adsorbed at equilibrium, mg/g
$q_m$	— Maximum adsorption quantity of $\text{Cu}^{2+}$ ion adsorbed by MHN, mg/g
$q_t$	— Quantity of $\text{Cu}^{2+}$ ion adsorbed at time $t$ , mg/g
$R$	— Ideal gas constant, 8.31 J/mol K
$R_L$	— Parameter related to the shape of Langmuir isotherm
$t$	— Contact time, min
$T$	— Kelvin temperature, K
$V$	— Wastewater bulk, L
$\Delta H$	— Change in enthalpy, kJ/mol
$\Delta S$	— Change in entropy, kJ/mol
$\Delta G$	— Change in standard free energy, kJ/mol

## References

- [1] World Health Organization, Guidelines for Drinking-Water Quality: Recommendations – Addendum, 3rd ed., Vol. 1, WHO Press, Geneva, 2008.
- [2] M. Ozmen, K. Can, G. Arslan, A. Tor, Y. Cengeloglu, M. Ersoz, Adsorption of Cu(II) from aqueous solution by using modified  $\text{Fe}_3\text{O}_4$  magnetic nanoparticles, *Desalination*, 254 (2010) 162–169.
- [3] K.A.S. Meraz, S.M.P. Vargas, J.T.L. Maldonado, J.M.C. Bravo, M.T.O. Guzman, E.A.L. Maldonado, Eco-friendly innovation for nejayote coagulation–flocculation process using chitosan: evaluation through zeta potential measurements, *Chem. Eng. J.*, 284 (2016) 536–542.
- [4] E.V. Soares, H.M.V.M. Soares, Cleanup of industrial effluents containing heavy metals: a new opportunity of valorizing the biomass produced by brewing industry, *Appl. Microbiol. Biotechnol.*, 97 (2013) 6667–6675.
- [5] H. Bai, Y. Kang, H. Quan, Y. Han, J. Sun, Y. Feng, Bioremediation of copper containing wastewater by sulfate reducing bacteria coupled with iron, *J. Environ. Manage.*, 129 (2013) 350–356.
- [6] D. DeNardis, D. Rosales-Yeomansa, L. Borucki, A. Philipossian, Studying the effect of temperature on the copper oxidation process using hydrogen peroxide for use in multi-step chemical mechanical planarization models, *Thin Solid Films*, 518 (2010) 3903–3909.
- [7] R. Molinari, P. Argurio, T. Poerio, Studies of various solid membrane supports to prepare stable sandwich liquid membranes and testing copper(II) removal from aqueous media, *Sep. Purif. Technol.*, 70 (2009) 166–172.
- [8] A. Jaiswal, S. Banerjee, R. Mani, M.C. Chattopadhyaya, Synthesis, characterization and application of goethite mineral as an adsorbent, *J. Environ. Chem. Eng.*, 1 (2013) 281–289.
- [9] M.A.A. Zaini, Y. Amano, M. Machida, Adsorption of heavy metals onto activated carbons derived from polyacrylonitrile fiber, *J. Hazard. Mater.*, 180 (2010) 552–560.
- [10] M.K. Uddin, A review on the adsorption of heavy metals by clay minerals, with special focus on the past decade, *Chem. Eng. J.*, 308 (2016) 438–462.
- [11] M. Harja, G. Buema, L. Bulgariu, D. Bulgariu, D.M. Sutiman, G. Ciobanu, Removal of cadmium(II) from aqueous solution by adsorption onto modified algae and ash, *Korean J. Chem. Eng.*, 32 (2015) 1–8.
- [12] M.W. Wan, C.C. Kan, B.D. Rogel, M.L.P. Dalida, Adsorption of copper (II) and lead (II) ions from aqueous solution on chitosan-coated sand, *Carbohydr. Polym.*, 80 (2010) 891–899.
- [13] J. Aguado, J.M. Arsuaga, A. Arencibia, M. Lindo, V. Gascon, Aqueous heavy metals removal by adsorption on amine-functionalized mesoporous silica, *J. Hazard. Mater.*, 163 (2009) 213–221.
- [14] T. Motsi, N.A. Rowson, M.J.H. Simmons, Adsorption of heavy metals from acid mine drainage by natural zeolite, *Int. J. Miner. Process.*, 92 (2009) 42–48.
- [15] M. Vila, S. Sánchez-Salcedo, M. Cicuéndez, I. Izquierdo-Barba, M. Vallet-Regí, Novel biopolymer-coated hydroxyapatite foams for removing heavy-metals from polluted water, *J. Hazard. Mater.*, 192 (2011) 71–77.
- [16] M.A. Hossain, H.H. Ngo, W.S. Guo, T.V. Nguyen, Palm oil fruit shells as biosorbent for copper removal from water and wastewater: experiments and sorption models, *Bioresour. Technol.*, 113 (2012) 97–101.
- [17] F.Z. Xie, F.C. Wu, G.J. Liu, Y.S. Mu, C.L. Feng, H.H. Wang, J.P. Giesy, Removal of phosphate from eutrophic lakes through adsorption by in situ formation of magnesium hydroxide from diatomite, *Environ. Sci. Technol.*, 48 (2014) 582–590.
- [18] X.N. Zhang, G.Y. Mao, Y.B. Jiao, Y. Shang, R.P. Han, Adsorption of anionic dye on magnesium hydroxide-coated pyrolytic biochar and reuse by microwave irradiation, *Int. J. Environ. Sci. Technol.*, 11 (2014) 1439–1448.
- [19] J.X. Lin, L. Wang, Adsorption of dyes using magnesium hydroxide-modified diatomite, *Desal. Wat. Treat.*, 8 (2009) 263–271.
- [20] X.J. Guo, J. Lu, L. Zhang, Magnesium hydroxide with higher adsorption capacity for effective removal of Co(II) from aqueous solutions, *J. Taiwan Inst. Chem. Eng.*, 44 (2013) 630–636.
- [21] J. Anwar, U. Shafique, W. Zaman, M. Salman, A. Dar, S. Anwar, Removal of Pb(II) and Cd(II) from water by adsorption on peels of banana, *Bioresour. Technol.*, 101 (2010) 1752–1755.
- [22] V.C.G.D. Santos, J.V.T.M.D. Souza, C.R.T. Tarley, J. Caetano, D.C. Dragunski, Copper ions adsorption from aqueous medium using the biosorbent sugarcane bagasse in natura and chemically modified, *Water Air Soil Pollut.*, 216 (2011) 351–359.
- [23] A. Polat, S. Aslan, Kinetic and isotherm study of copper adsorption from aqueous solution using waste eggshell, *J. Environ. Eng. Landscape Manage.*, 22 (2014) 132–140.
- [24] Y.J. Li, B.Y. Gao, T. Wu, D.J. Sun, X. Li, B. Wang, F.J. Lu, Hexavalent chromium removal from aqueous solution by adsorption on aluminum magnesium mixed hydroxide, *Water Res.*, 43 (2009) 3067–3075.
- [25] T.D. Pham, M. Kobayashi, Y. Adachi, Adsorption characteristics of anionic azo dye onto large  $\alpha$ -alumina beads, *Colloid. Polym. Sci.*, 293 (2015) 1877–1886.
- [26] E. Grzadka, Competitive adsorption in the system: carboxymethylcellulose/surfactant/electrolyte/ $\text{Al}_2\text{O}_3$ , *Cellulose*, 18 (2011) 291–308.
- [27] T.D. Pham, M. Kobayashi, Y. Adachi, Adsorption of anionic surfactant sodium dodecyl sulfate onto alpha alumina with small surface area, *Colloid. Polym. Sci.*, 293 (2015) 217–227.
- [28] J.R. Memon, S.Q. Memon, M.I. Bhangar, G.Z. Memon, A. El-Turki, G.C. Allen, Characterization of banana peel by scanning electron microscopy and FT-IR spectroscopy and its use for cadmium removal, *Colloids Surf., B*, 66 (2008) 260–265.
- [29] W. Konicki, D. Sibera, E. Mijowska, Z. Lendzion-Bielun, U. Narkiewicz, Equilibrium and kinetic studies on acid dye Acid Red 88 adsorption by magnetic  $\text{ZnFe}_2\text{O}_4$  spinel ferrite nanoparticles, *J. Colloid Interface Sci.*, 398 (2013) 152–160.
- [30] X. Sun, X. Huang, X.P. Liao, B. Shi, Adsorptive removal of Cu(II) from aqueous solutions using collagen-tannin resin, *J. Hazard. Mater.*, 186 (2011) 1058–1063.
- [31] W. Zheng, Y. Wang, L. Yang, X. Li, L. Zhou, Y. Li, Novel adsorbent of polymeric complex derived from chelating resin with Cu(II) and its removal properties for cyanide in aqueous solution, *Colloids Surf., A*, 455 (2014) 136–146.

- [32] Y.H. Liu, S. Kumar, J.H. Kwag, C.S. Ra, Magnesium ammonium phosphate formation, recovery and its application as valuable resources: a review, *J. Chem. Technol. Biotechnol.*, 88 (2013) 181–189.
- [33] I. Anastopoulos, G.Z. Kyzas, Composts as biosorbents for decontamination of various pollutants: a review, *Water Air Soil Pollut.*, 226 (2015) 1–16.
- [34] A. Celekli, M. Yavuzatmaca, H. Bozkurt, An eco-friendly process: predictive modelling of copper adsorption from aqueous solution on *Spirulina platensis*, *J. Hazard. Mater.*, 173 (2010) 123–129.
- [35] G. Issabayeva, M.K. Aroua, N.M. Sulaiman, Study on palm shell activated carbon adsorption capacity to remove copper ions from aqueous solutions, *Desalination*, 262 (2010) 94–98.
- [36] E. Igberase, P. Osifo, A. Ofomaja, The adsorption of copper (II) ions by polyaniline graft chitosan beads from aqueous solution: equilibrium, kinetic and desorption studies, *J. Environ. Chem. Eng.*, 2 (2014) 362–369.
- [37] P.T. Yeung, P.Y. Chung, H.C. Tsang, J.C.O. Tang, G.Y.M. Cheng, R. Gambari, C.H. Chui, K.H. Lam, Preparation and characterization of bio-safe activated charcoal derived from coffee waste residue and its application for removal of lead and copper ions, *RSC Adv.*, 73 (2014) 38839–38847.
- [38] B. Kizilkaya, A.A. Tekinay, Y. Dilgin, Adsorption and removal of Cu (II) ions from aqueous solution using pretreated fish bones, *Desalination*, 264 (2010) 37–47.
- [39] D. Nandi, T. Basu, S. Debnath, A.K. Gosh, A. De, U.C. Ghosh, Mechanistic insight for the sorption of Cd(II) and Cu(II) from aqueous solution on magnetic Mn-doped Fe(III) oxide nanoparticle implanted graphene, *J. Chem. Eng. Data*, 58 (2013) 2809–2818.